Postprint of: Blok M., Sample Rate Conversion Based on Frequency Response Masking Filter, 2018 International Conference on Signals and Electronic Systems (ICSES), 10-12.09.2018, Kraków, Polska, pp. 137-142, DOI: 10.1109/icses.2018.8507320

Sample Rate Conversion Based on Frequency Response Masking Filter

Marek Blok
Faculty of Electronics, Telecommunications and Informatics
Gdańsk University of Technology
Gdańsk, Poland
Marek.Blok@eti.pg.edu.pl

***Abstract*—The sample rate conversion with high resampling ratios requires low-pass digital filters with very narrow transition band which results in high computational complexity and makes filter design problematic. Therefore in this work we propose to use the FRM method, which breaks the filter with a narrow transition band into a group of filters with reduced design requirements. This decreases the number of non-zero coefficients and as a result the use of the FRM filter reduces the computational complexity of the resampler.**

Keywords—sample rate conversion, interpolator, decimator, resampling filter design, I-FIR filter, FRM filter

I. Introduction

In many digital signal applications it is convenient or necessary to change the sampling rate of the processed signal. In many cases such a task is relatively simple [1] and many sample rate conversion algorithms exist ([2], [3], [4], [5], [6], [7]), nevertheless, when the interpolation or decimation with high ratio is considered, then the resampling process requires digital lowpass filters with very narrow passband and transition band. Such requirements result in long impulse response which translates into high computational complexity of the interpolation or decimation algorithm. One of the solutions to this problem is the Frequency Response Masking (FRM) method ([8], [9]) which splits the resampling filter design problem into design of several filters with less demanding specifications. In the result the number of overall non-zero coefficients of the obtained filter structure is decreased which corresponds to lowered computational complexity of its implementation. In this paper the interpolator/decimator filter design with the use of FRM method is analyzed and the new structures of the interpolator and decimator based on the FRM filter are presented. It has been also demonstrated that the proposed structures allow for decrease in computational complexity in comparison to polyphase implementation of the interpolator or decimator with the resampling filter designed directly.

II. Classic Interpolator and Decimator

Fig. 1 presents classic interpolator and decimator. The first consist of up-sampler ($L\uparrow$) followed by the $1/L$-band lowpass filter $H_{LPF}(z)$. The up-sampler increases sample rate L times simply by inserting between every two input samples $L-1$ zeroes. On the other hand, the L-fold decimator (Fig. 1b) consist of the $1/L$-band lowpass filter $H_{LPF}(z)$ followed by the down-sampler, which for every L input samples discards $L-1$ samples.

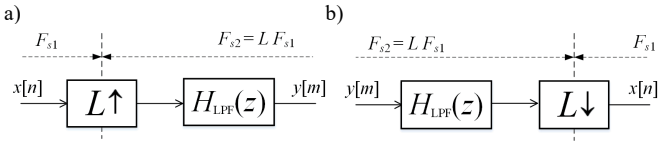

Fig. 1. Classic L-fold interpolator (a) and decimator (b).

The main advantage of these approaches is their simplicity. Nevertheless, if high fidelity of sample rate conversion is required then the impulse response of the lowpass resampling filter $H_{LPF}(z)$ becomes very long. Additionally, the resampling filter operates at higher sample rate $F_{s2} = L \cdot F_{s1}$ (in case of the interpolator this is the output sample rate and in case of the decimator this is the input sample rate), which results in very high computational complexity.

A. Polyphase Strutures

Let us notice that in the interpolator only every L-th input sample of the resampling filter is non-zero, while in the decimator all samples except every L-th output sample of the resampling filter are discarded. This means that most of the filter calculations can be omitted, which can be achieved with polyphase structures Fig. 2 ([2], [4], [5], [10], [11]) that have L-times lower computational complexity then the classic structures. In these structures the resampling filter is split into L polyphase subfilters with impulse responses:

$$g_i[n] = h_{LPF}[L \cdot n + i], \tag{1}$$

where $i = 0,1,\dots,L-1$ and $h_{LPF}[n]$ is an impulse response of the resampling filter. Notice, that L-fold interpolator and L-fold decimator can use the same resampling filter which means that they also can use the same polyphase filters.

Since in both polyphase structures the polyphase filters operate at the lowest sample rate, input sample rate for interpolator and output sample rate for decimator, the number of multiplications and additions, per input sample in the interpolator and per output sample in the decimator, in polyphase structures is equal to the length of the impulse response of the resampling filter.

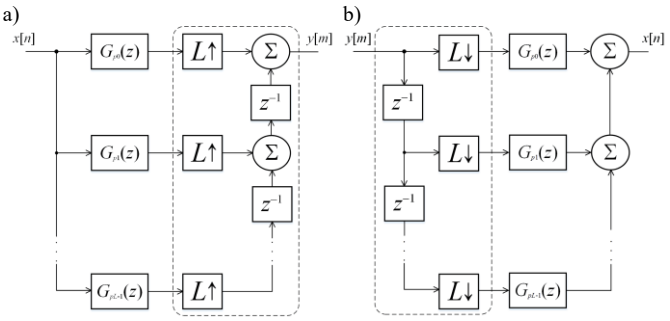

Fig. 2. Polyphase structures of the (a) interpolator and (b) decimator.

B. Resampling Filter

The up-sampler in the interpolator results in a signal with spectrum consisting of L replicas of the original spectrum. Since usually only the first, baseband, replica is needed, the Lth band lowpass filter is used to filter out the remaining replicas, which in the time domain results in the zeroes inserted by the up-sampler being replaced with the correct values of the interpolated signal. The down-sampler, on the other hand, results in the aliasing and the Lth band lowpass input filter is necessary to remove the input signal components that would be aliased. As it can be seen, the up-sampling and related down-sampling algorithms with corresponding specifications can use the same Lth band lowpass resampling filter. This also means that polyphase filters, in case of the polyphase structures, are also the same. The same filter is simply used in a different manner in these two algorithms.

Let us consider design of very high performance L-fold interpolator and decimator with $L = 16$. The performance of the resampler directly depends on the resampling filter for which we assume following specification: passband ripples ± 0.1 dB, attenuation in the stop band 100 dB and the center of transition band located at $F_{s1}/2 = 24$ kHz.

Let us assume that the upper frequency of the passband of the resampling filter is $F_{max} = 20$ kHz. These assumptions can be readily satisfied with the resampling filter of length $N_{LPF} = 379$, thus the computational complexity of the resampler is 379 multiplications and additions. Nonetheless, if the resampling algorithm performance requirements are increased significantly, for example selecting $F_{max} = 23.9$ kHz, then the estimated length of the impulse response of the resampling filter is as high as 15106, which, apart from very high computational complexity, results in difficulty of such filter design. For example Matlab script `firpm` takes log time to finish the design and the filter attenuation is just 85dB. This means that obtaining the filter fulfilling the specifications requires us to solve two problems: limitation of computational complexity and finding a design method that would allow effective design of the resampling filter.

III. FRM Filter

An interesting solution for the design of filters with very narrow transition band is the FRM method ([8], [9]). The FRM filter (Fig. 3) forms its frequency response in the transition band with the help of the lowpass prototype filter with K-times wider transition band, where K is an integer number selected by the designer. The K-fold narrowing of the transition band is achieved by increasing K-times delays of all the delayers in the structure of the prototype filter. The resulting shaping filter with transfer function $H_p(z^K)$ has exactly the same computational complexity as the prototype filter but its frequency response is a K-fold repetition of the K-times narrowed frequency response of the prototype filter. Now, it is enough to place the masking filter $H_{mp}(z)$ after the shaping filter to remove the excess replicas from its frequency response. In the basic variant, when the only baseband replica of the narrowed frequency response is retained, the FRM method simplifies to the I-FIR (*Interpolated FIR*) method ([12], [13]) offering the filter with the following transfer function:

$$H_{IFIR}(\mathrm{z}) = H_p(z^K) \cdot H_{mp}(z). \tag{2}$$

In turn, if we leave more than one replica of the narrowed frequency response of the prototype filter, obtaining the desired lowpass filter needs "patching" the gaps between these replicas. This problem is solved by adding the second branch in the FRM structure (Fig. 3) in which the second masking filter $H_{mc}(z)$ eliminates the excess replicas from the frequency response of the filter complementary to the shaping filter. The complementary filter ideally fills the gaps in the frequency response of the shaping filter and needs just one addition. With this approach the structure implements the filter with the following transfer function:

$$H_{FRM}(z) = H_p(z^K) \cdot H_{mp}(z) + \left(z_p^{-K\tau_p} - H_p(z^K)\right) \cdot H_{mc}(z), \tag{3}$$

where τ_p is the net delay of the prototype filter $H_p(z)$.

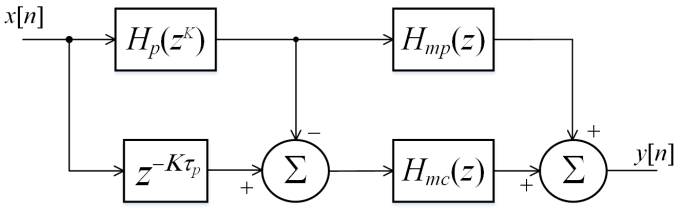

Fig. 3. FRM filter structure.

The FRM structure benefits from the fact that K-fold wider transition band of the prototype filter significantly decreases number of coefficients of its impulse response. Moreover, with properly selected K the width of transition bands of masking filters is also wider than the width of the transition band of the filter being designed. This decreases the complexity of component filters design and reduces the total number of non-zero coefficients of the structure, which in turn reduces the computational complexity of the FRM filter implementation.

A. Prototype Filter Specification

The main problem in FRM filter design is selection of the transition band location of the prototype filter. It is important that this band location must be selected in such a way that one of the transition bands of the shaping filter or the filter complementary to the shaping filter corresponds to the

assumed location of the transition band of the resampling filter being designed.

Let us assume that the transition band of the resampling filter is extracted from falling slopes of the frequency response of the shaping filter $H_p(z^K)$. Since the frequency response of the prototype filter is compressed and replicated the transition band of the shaping filter, which we are interested in, it is located in one of the ranges (f_p, f_s) with:

$$f_p = (i + f_{p,p})/K \text{ and } f_s = (i + f_{s,p})/K, \tag{4}$$

where $i = 0,1,2,\ldots$ ($i = 0$ in I-FIR case) and the range $(f_{p,p}, f_{s,p})$ determines the desired location of the transition band of the prototype filter. Thus, in this case, the edge frequencies of the prototype filter should be selected based on the following formulae:

$$f_{p,p} = K \cdot f_p - i \text{ and } f_{s,p} = K \cdot f_s - i, \tag{5}$$

where parameters K and i must be selected so that the following condition is met:

$$f_{p,p} < f_{s,p} \in (0,0.5). \tag{6}$$

Similarly, when we assume that the transition band of the resampling filter is extracted from falling slopes of the frequency response of the filter complementary to the shaping filter $H_p(z^K)$, which are the rising slopes of the shaping filter, the transition band of the shaping filter is located in the ranges (f_p, f_s) specified with the following formulae:

$$f_p = (i - f_{p,p})/K \text{ and } f_s = (i - f_{s,p})/K, \tag{7}$$

where $i = 1,2,\ldots$. From this the edge frequencies of the prototype filter should be selected based on the following formulae:

$$f_{p,p} = i - K \cdot f_p \text{ and } f_{s,p} = i - K \cdot f_s, \tag{8}$$

where K and i must result in fulfilling condition (6).

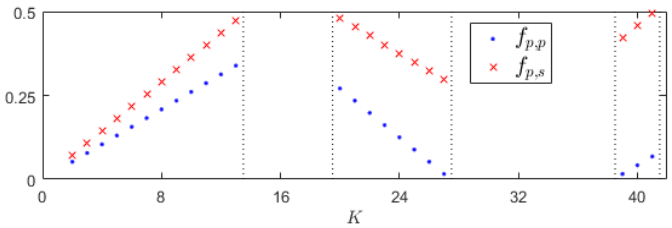

Fig. 4. Edge frequencies of the transition band of the prototype filter for different values of K parameter.

Now, let us consider the possible edge frequencies of the transition band of the prototype filter for both aforementioned cases for specification of the resampling filter given in sec. II.B with $F_{max} = 20$ kHz. Fig. 4 presents these frequencies in function of the parameter K. As we can see, the higher K is the wider transition band of the prototype filter becomes. Since edge frequencies tend to be pushed outside of the (0,0.5) range not all values of K are allowed (Fig. 4).

Apart from selecting edge frequencies of the prototype filter it is necessary to determine ripple size for its passband and stopband. The problem is that even though the use of the complementary shaping filter in the FRM structure does not require additional computations, it forces the use of the same ripple size in both passband and stopband. This is because the passband ripples in the shaping filter translate directly into stopband ripples in its complementary filter. At the same time, typically the required passband ripples of the resampling filter are significantly lower than the stopband ripples. This means that the limitation translates into increased requirements for the shaping filter and thus into larger number of coefficients of its impulse response. On the over hand, for the assumed maximum ripple size in the passband of the overall filter this allows to move the whole assumed ripples range to the requirements into the ripples size of the passband of the masking filters.

The exception to the above rule is the $i = 0$ case, that is the I-FIR filter case ([12], [13]), in which the complementary filter is not used. This allows independent selection of the ripple size in the passband and stopband of the prototype filter. Thus the specification for the prototype filter can be made less demanding on the expense of the masking filter specification.

B. Masking Filters Specifications

In Fig. 6 we can see magnitude responses of the shaping filter and its complementary filter for $K = 24$. For such K the transition band of the resampling filter is formed based on the first falling transition band of the shaping filter. Thus both masking filters need to pass the first passbands of the shaping and the complementary filters so the passband of the shaping filter fills the gap in its complementary filter. Nevertheless the filter masking the shaping filter $H_{mp}(z)$ has the narrower passband than the filter making the complementary filter $H_{mc}(z)$. It is also worth noticing that masking filter $H_{ma}(z)$ needs to preserve the shape of the last transition band of the shaping filter since it needs to stay being complementary to the first transition band of the filter complementary to the shaping filter. In case of the other masking filter, $H_{mc}(z)$, we do not need to be so strict, since the last transition band preserved by it will not have its complementary counterpart.

In this case, when the transition band is extracted from the filter complementary to the shaping filter (case presented in Fig. 6), the edge frequencies of transition band of the masking filter $H_{mp}(z)$ are specified as follows:

$$f_{p,mp} = \frac{2i-1}{K} - \frac{F_{max}}{L \cdot F_{s1}} \text{ and } f_{s,mp} = \frac{F_{max}}{L \cdot F_{s1}}, \tag{9}$$

which corresponds to the range from the end of the slope of the last preserved replica in the frequency response of the shaping filter till the beginning of the next replica, which at the same time is the beginning of the slope we want to preserve. Similarly, for the other masking filter, $H_{mc}(z)$:

$$f_{p,mc} = f_{s,mp} = \frac{F_{max}}{L \cdot F_{s1}} \text{ and } f_{s,mc} = \frac{2i}{K} - \frac{F_{p1} - F_{max}}{L \cdot F_{s1}}, \tag{10}$$

which corresponds to the beginning of the slope being preserved till the beginning of the next replica. The parameter i takes value determined during selection of the prototype filter specification.

By analogy, if the transition band is extracted from the shaping filter, the edge frequencies of the transition band of the masking filter $H_{mp}(z)$ are following:

$$f_{p,mp} = \frac{F_{max}}{L \cdot F_{s1}} \text{ and } f_{s,mp} = \frac{2i+1}{K} - \frac{F_{max}}{L \cdot F_{s1}}, \tag{11}$$

which corresponds to the range from the end of the preserved slope till the beginning of the next replica. In case of $H_{mc}(z)$ filter we get:

$$f_{p,mc} = \frac{2i}{K} - \frac{F_{max}}{L \cdot F_{s1}} \text{ and } f_{s,mc} = \frac{F_{max}}{L \cdot F_{s1}}, \tag{12}$$

which corresponds to the range from the end of the preserved replica till the next replica which is at the same time the beginning of the transition band of the filter being designed.

C. Design Example

In this subsection we will analyze the design example for the aforementioned specification of the resampling filter. Let us select $K = 24$ for which $i = 1$. The magnitude responses of the prototype filter $H_p(z)$ and its complementary filter $H_c(z)$ are presented in Fig. 5.

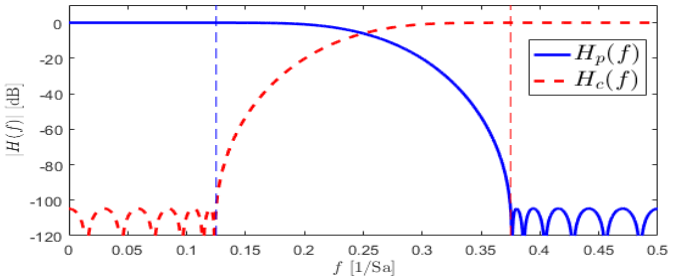

Fig. 5. Magnitude responces of the exemplary prototype H_p and complementary H_c filters.

Since the transition band is very wide, the length of the impulse response of the prototype filter is just $N_{prot} = 23$. Nevertheless, since the shaping filter and its complementary filter incorporate in the range (0, 0.5), $K/2$ replicas of the desired frequency response, masking filters are necessary (Fig. 6). This time, however, the transition bands of masking filters are more tighter and thus their impulse responses are significantly longer ($N_{ma} = 397$ and $N_{mc} = 199$).

Let us notice that in this case different transition band widths of the masking filters resulted in different impulse response length. This leads to masking filters delay disparity which needs to be compensated. Such compensation is a simple task if only the length for both masking filters are either even or odd. In such a case it is enough to add, before or after the shorter filter, the delayer with delay equal to:

$$\tau_c = \frac{|N_{ma} - N_{mc}|}{2}. \tag{13}$$

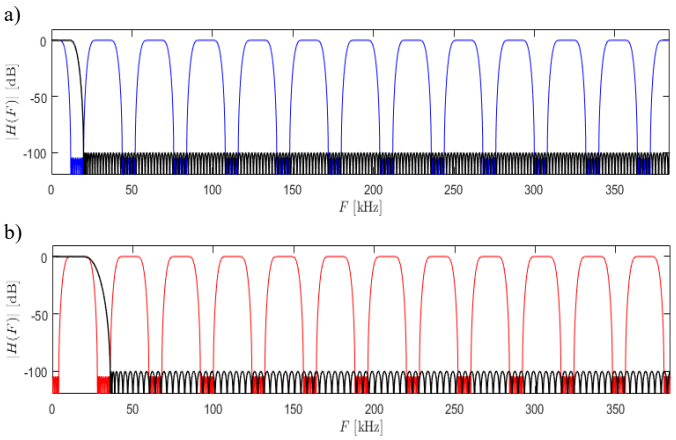

Fig. 6. Magnitude responses of shaping and masking filters for (a) a shaping filter and (a) a complementary filter for $K = 24$.

Nonetheless, let us notice that the frequency responses obtained in the upper and lower branches of the FRM filter (Fig. 7a) add up to the proper frequency response fulfilling our assumptions (Fig. 7b).

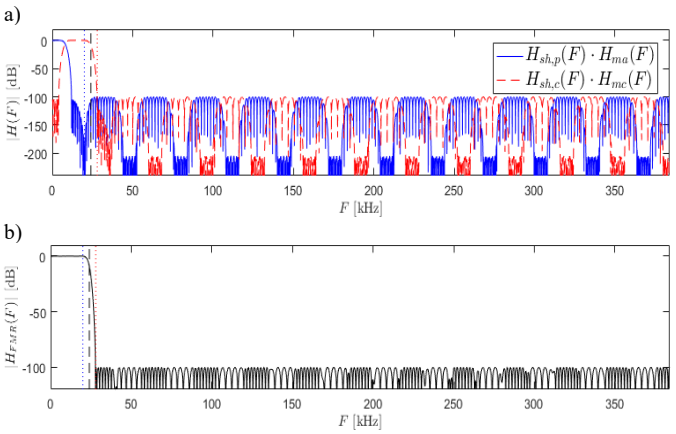

Fig. 7. Magnitude responses of upper and lower branch of (a) the FRM filter and (b) overall magnitude response of the FRM filter for $K = 24$.

D. FRM Structure Efficiency

If we consider overall number of coefficients $N_{all} = N_{prot} + N_{ma} + N_{mc} = 619$ of the FRM filter designed in the previous subsection we see that the number is actually one and a half times the number received for the direct design of the resampling filter where $N_{LPF} = 379$. In Fig. 8a we can see how the number of coefficients depends on the parameter K. Let us notice that although the $K = 24$ offers the almost the best results for FRM structure, the better results can be obtain for I-FIR structure, for example with $K = 8$ where the estimated overall number of coefficients $N_{all} = 124$. This is significant improvement when compared with direct resampling filter design, but to make resampler implementation based on such filter competitive to the polyphase structure the resampler using I-FIR filter needs to be restructured [14].

In Fig. 8 we can see that even though the increase of K parameter decreases the number of prototype filter coefficients, at the same time it results in more denser replicas in frequency response of the shaping filter, which in turn results in high

increase in number of coefficients of masking filters. Thus the benefits of the application of the FRM filter can be seen only if it is necessary to use the resampling filter with very narrow transition band as in Fig. 8b where $F_{max} = 23.9$ kHz.

This time the smallest number of coefficients $N_{all} = 1249$ ($N_{prot} = 585$, $N_{ma} = 330$ and $N_{mc} = 334$) is achieved for $K = 40$ (Fig. 8b). Now, this is not only more than 12 times less than the estimated length of the impulse response in the direct design $N_{LPF} = 15106$, but at the same time, contrary to the direct approach, the required FRM structure subfilters lengths allow easy design. Moreover, this effect is stronger if the transition band width decreases. The Fig. 9 presents overall magnitude response of the FRM filter designed for the aforementioned case.

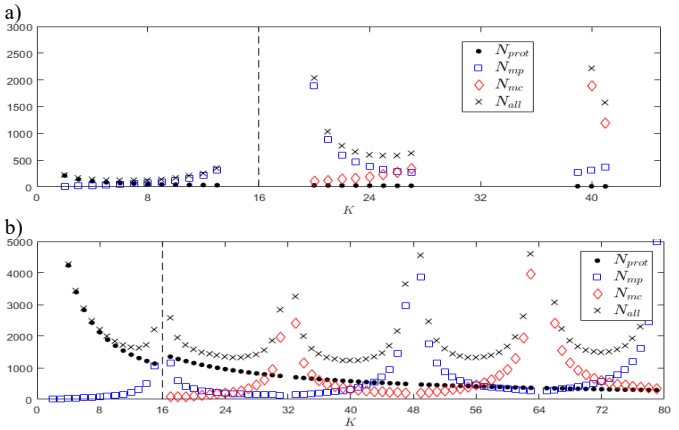

Fig. 8. The overall number of coefficients of the FRM structure N_{all} and its component filters (prototype filter N_{prot}, masking filter of the shaping filter N_{mp} and masking filter of the complementary filter N_{mc}) versus K for (a) $F_{max} = 20$kHz and (b) $F_{max} = 23.9$kHz.

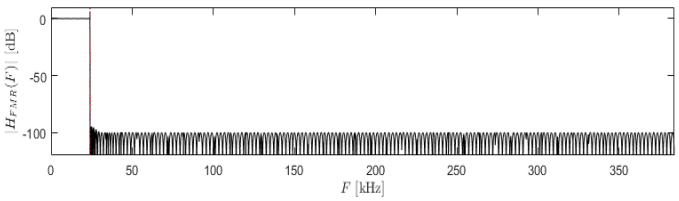

Fig. 9. Magnitude response of FRM filter with $F_{max} = 23.9$ kHz for $K = 40$.

IV. Resampling with FRM Filter

The goal of use of the FRM (or I-FIR) filter in a resampler is to decrease its computational complexity which can be related to a number of non-zero coefficients of the resampling filter. For example for $F_{max} = 20$kHz the lowest number of coefficients offers $K = 6$ (I-FIR case), for which $N_{all} = 114$. It must be noticed, however, that the use of the FRM filter, even if it offers lower number of coefficients, is not always a good choice. Nevertheless, as it has been mentioned before, if the resampling structure has to be competitive to the polyphase structures, it is necessary to redesign the resampler structure to utilize the properties of the I-FIR [14] or FRM filter [15]. In this case it means that it is better to use $K = 8$ with $N_{all} = 124$ because of the better relation between resampling coefficient $L = 16$ and parameter K. Since we cannot use K that is an integer multiple of L, the next best option is K that is equal to an integer multiple of $L/2$. Of course only integer values o K can be used.

This is similar with FRM filter structure, for which overall number of coefficients is close to local minima for $K = k \cdot L/2$ where $k = 1,3,5, \ldots$. In the next subsection the optimized structures of the FRM interpolator and decimator obtained for the aforementioned assumption are presented.

A. FRM Interpolator

The FRM interpolator structure [15] is presented in Fig. 10. The polyphase filters $G_{pi}(z)$ are obtained with twofold polyphase decomposition of $H_{prot}(z^{2K/L})$ filter whose impulse response contains $2K/L - 1$ zero valued samples between every pair of non-zero samples. Omitting calculation for zero valued samples of impulse responses of these filters and utilizing polyphase structures (Fig. 2a) in implementation of masking filters the proposed structure computational complexity is as low as:

$$\Theta = N_{prot} + N_{mc} + 2 \cdot \max(N_{ma}, N_{mc}) \qquad (14)$$

multiplications and additions per input sample. For example for the filter from Fig. 9 with $K = 40$ this number is $\Theta = 1587$. Which is almost ten times less than the computational complexity of polyphase implementation of the directly designed resampling filter of length $N_{LPF} = 15106$. Of course if such a filter was successfully designed.

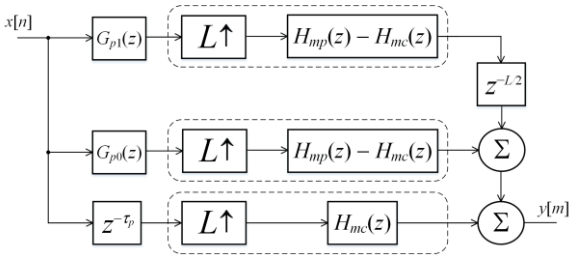

Fig. 10. Diagram of the interpolator based on the FRM filter.

B. FRM Decimator

The decimator structure corresponding to the interpolator shown in Fig. 10 can be readily obtained with its transposition. In the results we obtain the structure presented in Fig. 11 with the same subfilters as in the FRM interpolator. Since now the masking filters can be implemented using the polyphase decimator structure (Fig. 2b) the computational complexity of the proposed decimator structure is the same as in case of the interpolator.

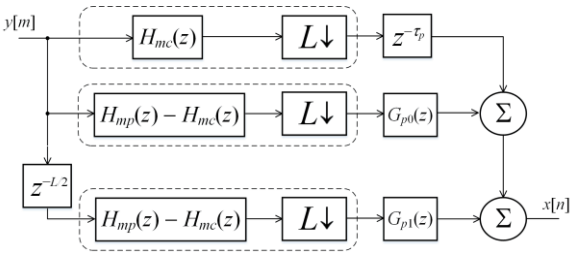

Fig. 11. Diagram of the decimator based on the FRM filter.

V. Conclusions

In this paper the problem of design of the resampling filter with narrow transition band has been discussed with relation to the FRM structure. It has been demonstrated that the FRM structure approach can be efficiently used only for very narrow transition bands. Nevertheless in such cases such an approach allows practical implementation of interpolator or decimator of very high sampling rate conversion performance requirements. The proposed approach results in significant decrease of coefficients number and with the proposed FRM interpolator and FRM decimator structures a high reduction in computational complexity can be obtained in comparison to the standard polyphase structures.

References

[1] J.S. Lim, A.V. Oppenheim (Eds.), Advanced Topics in Signal Processing, Prentice Hall, 1988.

[2] Y. C. Eldar, Sampling Theory: Beyond Bandlimited Systems. Cambridge University Press, 2015.

[3] P. Gupta, A. Verma, and R. Sharma., "A survey on efficient rational sampling rate conversion algorithms," Int. J. Sci. Res. Sci., Eng. and Technol., vol. 3(2), pp. 59-63, 2017.

[4] N. Hussain and S. Onkar, "Design and implementation of sampling rate converter using symmetric technique," Int. J. Eng. Sci. Comp., vol. 8(6), pp. 18509-18513, 2018.

[5] A. Kumar, S. Yadav, and N. Purohit, "Generalized rational sampling rate conversion polyphase FIR filter," IEEE Signal Process. Lett., vol. 24(11), pp. 1591-1595, 2017.

[6] D. Sinha, A.K. Verma, and S. Kumar, "Sample rate conversion technique for software defined radio receiver," IEEE 10th International Conference on Intelligent Systems and Control (ISCO), pp. 1-7, 2016.

[7] Y. Zhang and Y. Hao, "Analysis of sampling rate conversion technology in software radio," IEEE Advanced Information Management, Communicates, Electronic and Automation Control Conference (IMCEC), pp. 1812-1817, 2016.

[8] Y. Lim, "Frequency-response masking approach for the synthesis of sharp linear phase digital filters," IEEE Trans. Circuits Syst., vol. 33 (4), pp. 357-364, 1986.

[9] R. Bregovic, Y.C. Lim, and T. Saramaki, "Frequency response masking based design of two-channel FIR filterbanks with rational sampling factors and reduced implementation complexity," International Symposium on Image and Signal Processing and Analysis (ISPA), pp. 121-126, 2005.

[10] P.P. Vaidyanathan, Multirate Systems and Filter Banks, Prentice-Hall, Englewood Cliffs, 1993.

[11] A. Thakur, R. Mehra, and R. Kumar, "Computationally efficient sampling rate converter for audio signal application," IEEE 1st International Conference on Next Generation Computing Technologies (NGCT), pp. 567-570, 2015.

[12] R. Lyons, "Interpolated narrowband lowpass FIR filters," IEEE Signal Process. Mag, vol. 20 (1), pp. 50-57, 2003.

[13] T. Saramaki, T. Neuvo, and S.K. Mitra, "Design of computationally efficient interpolated FIR filters," IEEE Trans. Circuits Syst., vol. 35 (1), pp. 70-88, 1988.

[14] M. Blok, "Sample rate conversion with the use of I-FIR filter," in Polish, Przegląd Telekomunikacyjny i Wiadomości Telekomunikacyjne, No 8-9, pp. 1374-1379, 2011.

[15] M. Blok, "Interpolator based on frequency response masking filter," in Polish, Przegląd Telekomunikacyjny i Wiadomości Telekomunikacyjne, No 6, pp. 483-486, 2018.